Sparse Linear Equalizers for Turbo Equalizations in Underwater Acoustic Communication

Yanbo Wu*†, Min Zhu*†, and Xinguo Li†
*State Key Laboratory of Acoustics
Institute of Acoustics, Chinese Academy of Sciences, Beijing, China 100190
Email: wuyanbo@mail.ioa.ac.cn
†Ocean Acoustic Technology Center
Institute of Acoustics, Chinese Academy of Sciences, Beijing, China 100190

***Abstract*—Underwater acoustic channels are characterized by a time-varying multipath structure with a long delay spread. The multipath is usually very sparse. Direct-adaptation based turbo equalizer is a low-complexity and effective method to combat the inter-symbol interference caused by the time-varying multipath. This paper studies the determinations of the tap positions of the linear equalizers in the direct-adaptation multichannel turbo equalizer. A multiple threshold and retraining scheme is proposed to determine the sparse position of direct-adaptive equalizer in turbo equalization. The length of the training can be less than the number of the full taps. The performance of the proposed scheme is comparable to that of the scheme based on the orthogonal matching pursuit (OMP) algorithm, but much simpler. The proposed scheme is verified in the shallow ocean experiments at a distance of 5.3 km to transmit a bit rate of 4 bps.**

I. Introduction

In the shallow-water long-distance communication channel with an adverse sound speed profile, the acoustic signal is propagating with several reflections from the surface or the bottom, causing the low signal-to-reverberation ratio and the long delay spread [1]. The multichannel turbo equalization [2], [3] is a powerful means to work with a low signal level. For the long delay spread, to reduce the computation complexity and improve the channel estimation accuracy, the channel sparse characteristic [1] can be used to avoid overparameterization. The problem of optimizing the sparse support is NP-hard, and there are various methods to research the suboptimal solutions. The focus of this paper is on the sparse turbo equalizer from the perspective of implementation.

For the turbo equalization under long delay spread channels, the soft-in soft-out (SISO) equalizer is optimized based on the minimum mean square error (MMSE) criterion. The linear equalizer (LE) MMSE SISO equalizer works better than the decision-feedback equalizers (DFE) MMSE SISO equalizer, as the latter is less robust in the low signal-to-noise-ratio (SNR) condition. According to estimate the channel explicitly or implicitly, the MMSE-based turbo equalizations can be divided into: the channel-estimation-based turbo equalization and the direct-adaptive one, respectively. The channel-estimation-based SISO equalizer [4] is optimal in the SISO MMSE sense, however matrix inversion is needed to update the equalizer's coefficients. The practical equalizer based on channel estimation is updated per block, which restricts its channel tracking ability. The direct-adaptive SISO equalizer has a low computation complexity and a fast-tracking ability [3]. Although the *a priori* symbol variances from the SISO channel decoder are disregarded in the direct-adaptive SISO e-qualizer, the performance degradation in the equalizer's steady state is neglectable. From the perspective of the application of underwater acoustic communication and the computation complexity, the direct-adaptive SISO equalizer is more practical.

Acquiring and utilizing the sparse structure of the underwater acoustic channel for communication [3], [5]–[8] has been studied for over two decades, and is still an interesting area. In [5], the sparse channel estimation is obtained by magnitude threshold on the full channel estimation, and the feedforward filter of the DFE equalizer is with the same sparse structure of the channel estimation, according to the matched-filter properties. The sparse equalization technique in [5] was extend to the direct-adaptive turbo equalization [3]. In [8], the sparse channel estimation is used to cancel the post-cursor inter-symbol-interference prior to linear equalization. The delay-Doppler spread sparse estimation was developed in [7] to capture the dynamics of the time-varying sparse channels, such as underwater acoustic channel with significant surface waves, and the matching-pursuit (MP) based algorithms were applied to estimate the channel delay-Doppler-spread function. The channel sparsity in the time and/or Doppler domain also are exploited for a multicarrier underwater acoustic system [6].

The previous methods of the sparse equalizer for underwater acoustic communication, as we known, are based on the sparse channel estimation. Although the sparse channel estimation based on magnitude threshold is optimal in the MMSE sense, the equalizer sparse technique based on the matched-filter properties is suboptimal. Firstly, in the MMSE optimal solution, the equalizers (LE or DFE) for sparse channels in MMSE sense are not sparse [9]. Secondly, as the multichannel technique is usually used in underwater, the sparse pattern of the equalizer need to be jointly selected among the receiving channels. In [9], a design framework for sparse FIR multichannel equalizers was proposed, where greedy or convex-optimization algorithms can be used to obtain the sparse structure of the multichannel equalizer. However, it faces the contradiction of the tracking speed and the computational complexity. From the practical perspective, we seek to use the direct-adaptive method for sparse multichannel turbo equalization. In [10], the direct-adaptive sparse equalization problem was exploited under the compressive sensing perspective. Expect [10], the direct-adaptive sparse equalization problem has been seldom addressed.

978-0-933957-43-5 ©2015 MTS

In this paper, we propose a new scheme for the problem of direct-adaptive sparse equalization in turbo equalization. To reduce the computational complexity, the taps are updated by the the normalized least mean squares (NLMS) algorithm. When the multichannels of the equalizer are jointly sparselized, the train-data is reused, and the threshold of the equalizer's taps is gradually strict. The length of the training can be less than the number of the full taps. Compared with other algorithms, our scheme is easier for implementation, as it is close to the ordinary adaptive equalizer. The proposed scheme is used for the turbo equalization for the shallow-water long-distance communication, where the direct path is disappear and the signal-to-noise ratio (SNR) is low. After resampling to compensate the average Doppler shifting, the sparse pattern of the channel impulse response (CIR) is quasi-constant and the tap coefficients are fluctuating. The algorithm can also be applied to the short-distance communication, where the direct path is strong and the SNR is high, the in-direct paths with significantly different Doppler shifting are treated as interferences.

II. Channel and System Description

A. Shallow-water Long-Distance Channel

The channel impulse response (CIR) in the underwater acoustic channel is time-varying and with large delay spread. The delay profile is usually sparse with multiple clusters. The time-varying characteristic is scaled by the Doppler spread, which is effected by the motions of the transmitter/receiver and the surface. The multipaths may have different Doppler shifting, depending on the departure and arrival angles. For the shallow-water short-distance communication [7], where the horizontal distance is comparable with the water depth, the angles of the direct path and the surface-bottom reflection paths are quite different, leading to the Doppler shifting differences of the paths. Therefore, the sparse estimation of the delay-Doppler-spread function was used to distinguish the paths [7]. For long-distance communication, where the distance may be tens or hundreds of the water depth, the acoustic rays are near horizontal, leading to a narrow Doppler spread. The multipaths have a common Doppler shifting. In this paper, we consider the long-distance communication. After resampling to compensate the Doppler shifting, the sparse pattern of the channel delay spread is constant in short-time.

The channel measurements were based on the communication experiment in the South China Sea in 2013, during which the encoded data was modulated in quadric phase-shift keying (QPSK) with a symbol rate of 4 k symbols/s at a carrier frequency of 8 kHz. The water depth was 75 m, and the distances were 1.7 to 5.3 km. The receiver boat was anchored, and the transmitter boat was drifting by wind. The detail descriptions are in Sect. IV. To obtain a high resolution in Doppler spread, the data length was 7 s, much longer than that in [7], therefore the Doppler effect causes not only the carrier frequency shifting but also the drift of the symbol sampling. The sample is matched with the delayed and resampled versions of the transmitted sequence. To match the received waveform under the Doppler scaling factor Δ [14], the local vector is generated from the transmitted bandpass waveform in a sampling interval of $(1+\Delta)T_s$, where T_s is the standard sampling interval in the receiver.

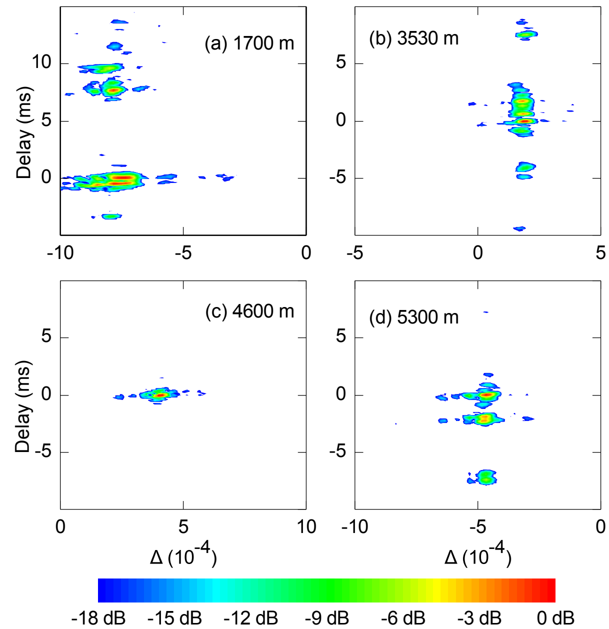

Fig. 1. Delay-Doppler-spread functions at different distances in the shallow ocean experiment. The Doppler spread is scaled by the Doppler scaling factor Δ. The sample is matched with the delayed and resampled versions of the transmitted sequence.

Fig. 1 shows the delay-Doppler-spread functions at different distances in the shallow ocean experiment. It can be seen that the delay spread is sparse, and the main Doppler shiftings of different paths are nearly the same. For Fig. 1-(a) with a shortest distance, the Doppler spread is generally larger than that with other distances, due to that the paths are more inclined. The 6-dB width of the Doppler spread is less than 10^{-4}, which is benign for tracking the taps by the adaptive filters after resampling. Fig. 2 shows the time-varying CIR at the distance of 5300 m after resampling for to compensate the main Doppler. The CIR was estimated at the beginning of each frame (the frame interval is 630 ms, 12 frames). It can be seen that the sparse pattern of the delay spread is nearly constant between adjacent frames, and the tap magnitudes are slowly fluctuating. The width of each cluster in delay spread is about 0.5 ms, the duration of two symbols.

B. Transmitter Description

The transmitter structure is based on turbo code and quaternary phase shift keying (QPSK) modulation, as shown in Fig. 3. First, the information bits are encoded by a rate $\frac{1}{2}$ turbo encoder, producing the coded bit sequence. The sequence is permuted using a random interleaver and then mapped to QPSK symbols.

The frame structure, as shown in Fig. 4, consists the linear frequency modulation (LFM) signal, the training symbols followed by the data symbols. The LFM signals and the blanks are inserted between the symbol sequences for the time and Doppler synchronization purposes. The periods of training and data sequences are N_t and N_d symbol times, respectively.

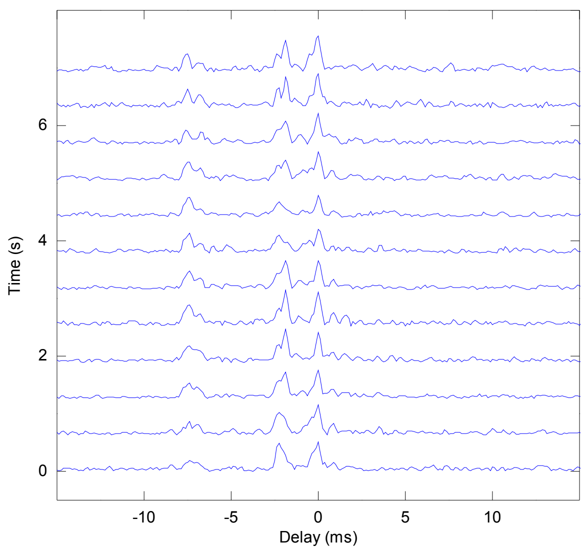

Fig. 2. Time-varying channel impulse response after Doppler compensation at the distance of 5300 m.

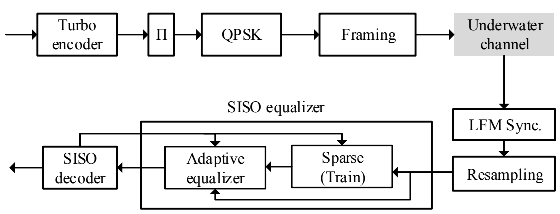

Fig. 3. Transmitter and receiver structures.

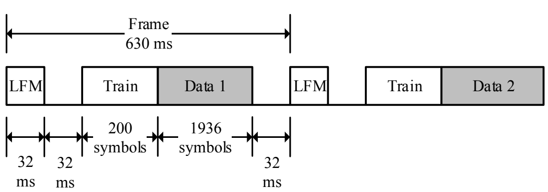

Fig. 4. Frame structure.

III. Direct-adaptive Sparse SISO LE

We use the complex-valued equivalent baseband signal model. Assuming an oversampling factor of N_s, the signal received at the j^{th} hydrophone $(1 \leq j \leq N_r)$ at time n is expressed as [3]

$$\mathbf{r}_n = \sum_{k=-N_f}^{N_p} \mathbf{H}_{n,k} x_{n-k} + \mathbf{w}_n \tag{1}$$

where k is the delay index. Note that $\mathbf{r}_n$, $\mathbf{H}_{n,k}$ and $\mathbf{w}_n$ are the $N_s N_r \times 1$ received sample vector, channel impulse response vector and noise vector, respectively. The channel length is assumed to be at most $N_f + N_b + 1$, where N_f and N_p are the lengths of the percursor and postcursor responses, respectively. Considering an observation window containing $L_f + L_b + 1$ received vectors, i.e., $\mathbf{r}_{n-L_p}, \cdots, \mathbf{r}_{n+L_f}$, we can write

$$\mathbf{y}_n = \mathbf{H}_n \mathbf{x}_n + \mathbf{n}_n \tag{2}$$

where

$$\mathbf{y}_n = \left[\mathbf{r}_{n+L_f}^{\mathrm{T}}, \cdots, \mathbf{r}_{n-L_p}^{\mathrm{T}}\right]^{\mathrm{T}}$$
$$\mathbf{n}_n = \left[\mathbf{w}_{n+L_f}^{\mathrm{T}}, \cdots, \mathbf{w}_{n-L_p}^{\mathrm{T}}\right]^{\mathrm{T}}$$
$$\mathbf{x}_n = \left[x_{n+L_f}, \cdots, x_{n-L_p}\right]^{\mathrm{T}}$$

and $\mathbf{H}_n =$

$$\begin{bmatrix} \mathbf{H}_{n+L_f,-K_f} & \cdots & \mathbf{H}_{n+L_p,K_p} & \mathbf{0} & \mathbf{0} \\ \mathbf{0} & \ddots & \cdots & \ddots & \mathbf{0} \\ \mathbf{0} & \mathbf{0} & \mathbf{H}_{n-L_p,-K_f} & \cdots & \mathbf{H}_{n-L_p,K_p} \end{bmatrix}$$

The SISO equalizer produces extrinsic log-likelihood ratios (LLR) of the coded bits using the received vector $\mathbf{y}_n$ and the *a priori* LLRs. For direct adaptive SISO equalizer, the *a priori* LLRs are converts into the *a priori* symbol means $\bar{x}_n$, and the symbols are estimated using the received vector and the *a priori* mean vector as follows

$$\hat{x}_n = \mathbf{f}_n^{\mathrm{H}} \mathbf{y}_n + \mathbf{g}_n^{\mathrm{H}} \bar{\mathbf{x}}_n \tag{3}$$

where $\bar{\mathbf{x}}_n = \left[\bar{x}_{n+L_f}, \cdots, \bar{x}_{n-1}, \bar{x}_{n+1}, \cdots, \bar{x}_{n-L_p}\right]^{\mathrm{T}}$. The $\mathbf{f}_n$ and $\mathbf{g}_n$ are coefficient vectors of the feedforward and feedback filters, and updated by adaptive algorithms. The extrinsic LLRs are then calculated based on the sequences $\{\hat{x}_n\}$ and feed into the SISO decoder.

A. Sparsing by multiple threshold method

A multiple-threshold-retraining scheme is proposed for the direct-adaptive sparse SISO LE. The threshold-retraining method was firstly proposed in [11] as the sparse least-square (LS) algorithm , where reestimation is carried out after thresholding. The performance of sparse LS is close to that of the matching pursuit (MP) algorithm and the sparse LS is quite less complexity. As a variant of LS, it also meets the problem of overparameterization, and the requirement that the size of training vector is larger than that of the input vector can not be satisfied in the direct form of the multichannel equalizer. From the observation of the adaptive equalizer with insufficient training, we find that although the tap magnitudes are far from convergence, the sparse pattern of the equalizer can be obtained. Therefore, we extend the sparse LS algorithm to the adaptive algorithm and use multiple thresholds to reuse the limited training symbols.

The proposed algorithm is shown in Algorithm 1. The algorithm is applicable for both the initial iteration and the subsequent iterations, leading to different values of the input vector $\mathbf{d}_n$ and the target value x_n. For the initial iteration, $\mathbf{d}_n = \mathbf{y}_n$, and $x_n (N_t < n \leq N_d)$ takes the value of the equalizer's hard decision. For the subsequent iterations where the decoder feedback is available, $\mathbf{d}_n = \left[\mathbf{y}_n^{\mathrm{T}}, \bar{\mathbf{x}}_n^{\mathrm{T}}\right]^{\mathrm{T}}$, and $x_n (N_t < n \leq N_d)$ is replaced by the hard decision based on the decoder's output $\bar{x}_n$.

Fig. 5 shows the sparse training process using the proposed algorithm. The feedfoward filter of each channel covers 80 symbols, the over sampling factor and the number of the receiving hydrophones are $N_s = 2, N_r = 4$, respectively, therefore, the length of the input vector is 640, which is larger than the training length $N_t = 200$. The multiple thresholds are

Algorithm 1 multiple-threshold-retraining adaptive equalizer

The sparse taps are retrained in NLMS and selected with multiple thresholds $[\lambda_1 \cdots \lambda_{N_\lambda}]$, and the sparse pattern is expanded to N_e symbols of both sides. The initializations are as follows: $\mathbf{s}_0 = \mathbf{1}$, $\mathbf{w}_0 = \mathbf{0}$, and $i = 0$.

1) *Training:* For $1 \le n \le N_t$:

$$\begin{aligned}\hat{x}_n &= \mathbf{w}_n^{\mathrm{H}}\mathrm{Diag}\{\mathbf{s}_i\}\mathbf{d}_n \\ e_n &= x_n - \hat{x}_n \\ \mathbf{w}_{n+1} &= \mathbf{w}_n + \mu\frac{\mathrm{Diag}\{\mathbf{s}_i\}\mathbf{d}_n}{\|\mathrm{Diag}\{\mathbf{s}_i\}\mathbf{d}_n\|^2}e_n.\end{aligned}$$

2) *Threshold:*

$$\begin{aligned}i &= i+1 \\ \mathbf{s}_i &= \frac{|\mathbf{w}_{N_t}|}{\max\{|\mathbf{w}_{N_t}|\}} > \lambda_i\end{aligned}$$

if $i < N_\lambda$: go to step 1); else go to step 3).

3) *Sparsity expansion:*

$$b_j^{(i)} = \mathrm{OR}([a_j^{(i-N_sN_e)} \dots a_j^{(i+N_sN_e)}])$$

where $a_j^{(i)}$ and $b_j^{(i)}$ are the i^{th} element from the j^{th} channel of $\mathbf{s}_{N_\lambda}$ and $\mathbf{s}$, respectively, and the OR() is the binary-OR-operator of all the elements.

4) *Sparse adaptive equalizer:* For $1 \le n \le N_t + N_d$

$$\begin{aligned}\hat{x}_n &= \mathbf{w}_n^{\mathrm{H}}\mathrm{Diag}\{\mathbf{s}\}\mathbf{d}_n \\ e_n &= x_n - \hat{x}_n \\ \mathbf{w}_{n+1} &= \mathbf{w}_n + \mu\frac{\mathrm{Diag}\{\mathbf{s}\}\mathbf{d}_n}{\|\mathrm{Diag}\{\mathbf{s}\}\mathbf{d}_n\|^2}e_n.\end{aligned}$$

selected as $[\lambda_1, \lambda_2, \lambda_3] = [0.1, 0.2, 0.4]$, the expansion length after the final threshold is $N_e = 3$, and the adaptive step in NLMS is $\mu = 0.25$. We can see the differences of the sparse pattern between the four channels. The number of the selected taps is 217. Fig. 6 shows the tap magnitudes in the decision-directed mode during one frame. It is shown the maximum position in each cluster is slowly sliding, which testifies the necessity of the sparsity expansion step in Algorithm 1.

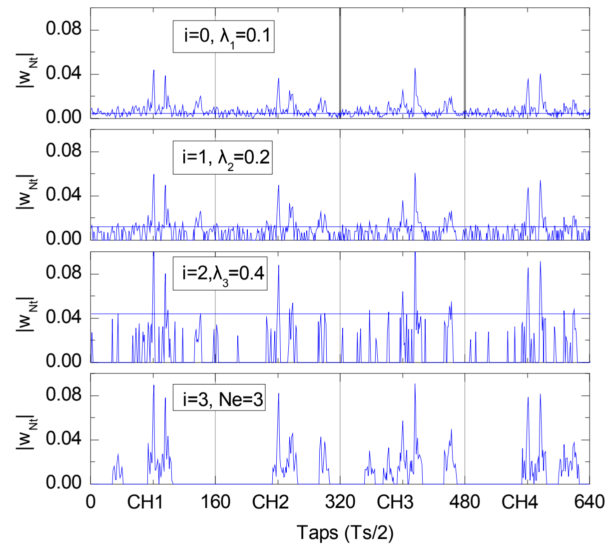

Fig. 5. The sparse training of the 4-channel equalizer and the varying thresholds of the tap magnitudes (at the distance of 5300 m, 200 training symbols, double symbol-rate sampling). The taps are iteratively sparselized by retraining with the same receiving samples and selected with the thresholds [0.1, 0.2, 0.4] of the maximum magnitude. In considering the channel fluctuation, the sparse positions in each channel are finally expanded with adjacent 3 symbols.

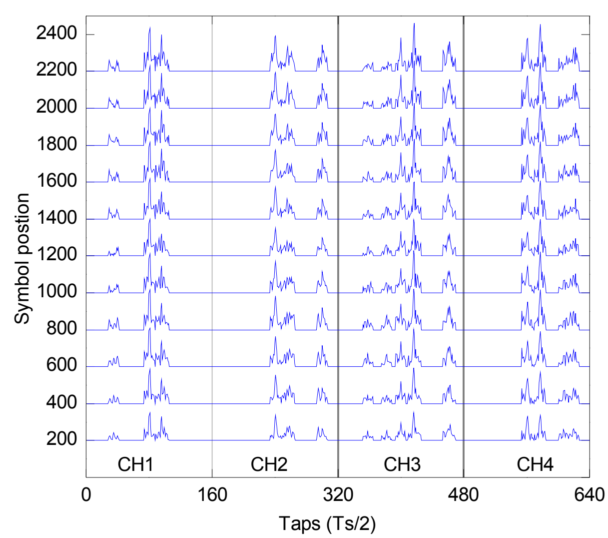

Fig. 6. The tap magnitudes of the 4-channel sparse equalizer in the decision-directed mode at the distance of 5300 m. One frame contains 200 training symbols and 2136 data symbols.

B. Sparsing by channel-estimation-based and OMP

As a comparison, the channel-estimation-based sparse equalizer is also studied. The SNR requirement in turbo equalization is lower than the DFE scheme, therefore the sparse processing of the noisy estimation of CIR may lead to performance degradation. We use the framework of the sparse equalizer proposed in [9], where the sparse equalizer is selected by the orthogonal matching pursuit (OMP) algorithm based on the non-sparse channel estimation. After the sparse

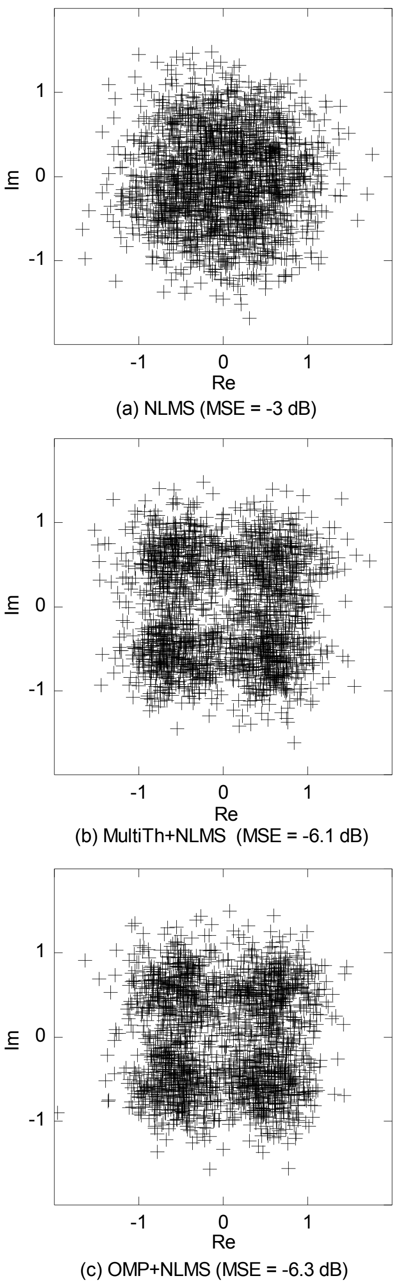

Fig. 7. Scatter plots of the adaptive equalizers with different sparsing algorithms.

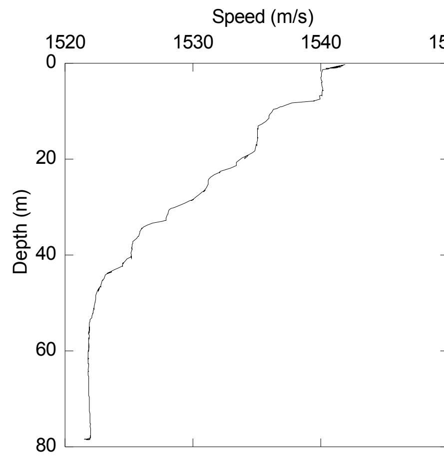

Fig. 8. Sound speed profile in South China Sea at 10:52 on August 30, 2013.

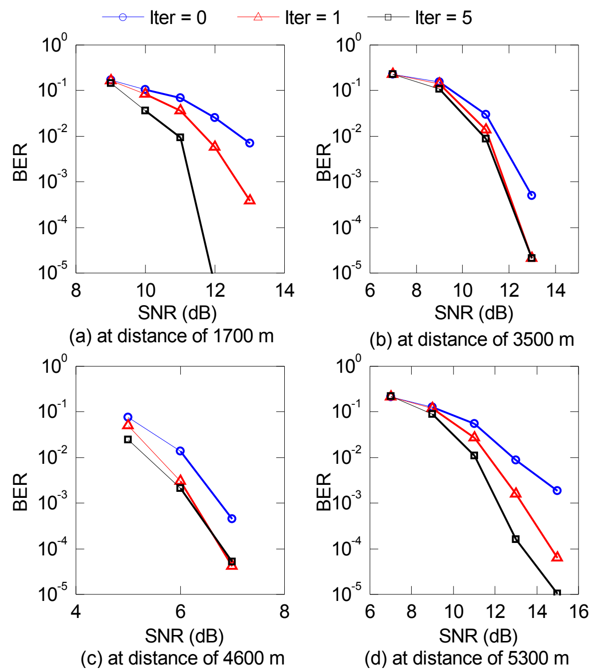

Fig. 9. BER performances of adaptive turbo equalization based on proposed sparse algorithm.

pattern of the multichannel equalizer is obtained, we start equalising from the start of the frame as step 4) in Algorithm 1. The steps are briefly list as follows:

- Step 1): estimating the each CIR by LS with the training samples, and estimating the noise variances;
- Step 2): Calculating the correlation matrix $\mathbf{R}_{yy}$ and $\mathbf{R}_{yx}$, and making Cholesky factorization $\mathbf{R}_{yy} = \mathbf{L}\mathbf{L}^{\mathrm{H}}$;
- Step 3): Solving the optimization program by OMP algorithm.

$$\min \|\mathbf{w}_s\|_1 \quad \text{s.t.} \;\; \|\mathbf{L}^{\mathrm{H}}\mathbf{w}_s - \mathbf{L}^{-1}\mathbf{r}_{\Delta}\|_2^2 \leq \epsilon$$

where $\mathbf{r}_{\Delta}$ is a specific column of $\mathbf{R}_{yx}$, and the column position is determined by the equalizer's delay;
- Step 4): NLMS equalizing the frame with the sparse pattern from $\mathbf{w}_s$ in last step.

Different sparse algorithms are used to equalize the frame at the 5300 m distance. The scatter plots of the the full-tap adaptive equalizer, the proposed scheme and the OMP-based adaptive equalizer are shown in Fig.7. The tap vector size in the full-tap equalizer is 640, larger than the length of the training symbols, leading to the divergence in decision-directed mode. By the proposed sparse algorithm, the size of the feedfoward vector in the equalizer is reduced to 217, which is also used as the stop criteria of the OMP algorithm. Although a larger training length is required to obtain full convergence, the mean square errors (MSE) of both the proposed algorithm and the OMP-based one are less than -6 dB, which is sufficient for the turbo decoding. The OMP-based algorithm has a slightly better performance, however its computation complexity is much higher.

IV. Ocean Experiments

The experiments were carried out in August, 2013 in the South China Sea. The sound speed profile is shown in Fig.8. The transducer was lowed from a moving boat to the depth of 15 m. The 4-element hydrophone array was lowed from an anchored boat, at separated depths from 13 m to 15 m. In each frame, the 1936 information bits was encoded by a half-rate turbo encoder whose mother code is the recursive systematic convolutional code $(23, 35)_{\mathrm{OCT}}$. The QPSK symbol rate was 4 kBaud, and the carrier frequency was 8 kHz. The multichannel waveforms were sampled at a clock of 64 kHz, and then added Gaussian noise with different levels.

The performance of adaptive linear turbo equalization based on the proposed algorithm is shown is Fig.9. The maximum iteration is 5. The SNR requirement at the distance of 4600 m is the lowest, which agrees with that the 4600 m channel is nearest to the AWGN channel as shown in Fig.1. The iteration gain is obvious in the severe multipath channels.

V. Conclusion

A multiple threshold and adaptive retraining scheme has been proposed to determine the sparse position of direct-adaptive equalizer in turbo equalization. The sparse pattern based on the proposed algorithm is near to the OMP algorithm. With the sparse structure, the NLMS equalizer can be used with limited number of the training symbols in turbo equalization in the underwater communication system.

Acknowledgment

This work is supported by the National Natural Science Foundation of China under Grant No. 61471351.

References

[1] M. Stojanovic, and J. Preisig, "Underwater acoustic communication channels: propagation models and statistical characterization," *IEEE Commununication Magzine*, vol. 47, pp. 84–89, Jan 2009.

[2] A. C. Singer, J. K. Nelson, and S. S. Kozat, "Signal processing for underwater acoustic communications," *IEEE Communications Magazine*, vol. 47, pp. 90–96, 2009.

[3] J. W. Choi, T. J. Riedl, K. Kim, A. C. Singer, and J. C. Preisig, "Adaptive Linear Turbo Equalization Over Doubly Selective Channels," *IEEE Journal of Oceanic Engineering*, vol. 36, pp. 473–489, Oct 2011.

[4] R. Otnes and M. Tüchler, "Iterative channel estimation for turbo equalization of time-varying frequency-selective channels," *IEEE Transactions on Wireless Communications*, vol. 3, pp. 1918–1923, 2004.

[5] M. Kocic, D. Brady, and M. Stojanovic, "Sparse equalization for real-time digital underwater acoustic communications," in *Proc. MTS/IEEE OCEANS*, 1995, vol. 3, pp. 1417–1422.

[6] C. R. Berger, S. Zhou, J. C. Preisig, and P. Willett, "Sparse channel estimation for multicarrier underwater acoustic communication: from subspace methods to compressed sensing," *IEEE Transactions on Signal Processing*, vol. 58, pp. 1708–1721, Mar 2010.

[7] W. Li and J. C. Preisig, "Estimation of rapidly time-varying sparse channels," *IEEE Journal of Oceanic Engineering*, vol. 32, pp. 927–939, Oct 2007.

[8] M. Stojanovic, L. Freitag, and M. Johnson, "Channel-estimation-based adaptive equalization of underwater acoustic signals", in *Proc. MTS/IEEE OCEANS*, 1999, vol. 2, pp. 985–990.

[9] A. Gomaa and N. Al-Dhahir, "A new design framework for sparse fir mimo equalizers," *IEEE Transactions on Communications*, vol. 59, pp. 2132–2140, Aug 2011.

[10] E. Vlachos, A. S. Lalos, and K. Berberidis, "Stochastic gradient pursuit for adaptive equalization of sparse multipath channels," *IEEE Journal on Emerging and Selected Topics in Circuits and Systems*, vol. 2, pp. 413–423, Sep 2012.

[11] S. F. Cotter and B. D. Rao, "Sparse channel estimation via matching pursuit with application to equalization," *IEEE Transactions on Communications*, vol. 50, pp. 374–377, Mar 2002.

[12] M. Tüchler, R. Koetter, and A. C. Singer, "Turbo equalization: Principles and new results," *IEEE Transactions on Communications*, vol. 50, pp. 754–767, 2002.

[13] R. A. Iltis, "Iterative joint decoding and sparse channel estimation for single-carrier modulation," in *Proc. of Intl. Conf. on Acoustics, Speech and Signal Proc.*, Las Vegas, NV, Apr. 2008, pp. 2689–2692.

[14] K. Tu, T. M. Duman, M. Stojanovic, and J. G. Proakis, "Multiple-resampling receiver design for OFDM over Doppler-distorted underwater acoustic channels," *IEEE Journal of Oceanic Engineering*, vol. 38, pp. 333–346, Apr 2013.